Title:

Release of mineral-bound water prior to subduction tied to shallow seismogenic slip off Sumatra

Authors:

Andre Hüpers[1*], Marta E. Torres[2], Satoko Owari[3], Lisa C. McNeill[4], Brandon Dugan[5], Timothy J. Henstock[4], Kitty L. Milliken[6], Katerina E. Petronotis[7], Jan Backman[8], Sylvain Bourlange[9], Farid Chemale, Jr.[10], Wenhuang Chen[11], Tobias A. Colson[12], Marina C.G. Frederik[13], Gilles Guèrin[14], Mari Hamahashi[15], Brian M. House[16], Tamara N. Jeppson[17], Sarah Kachovich[18], Abby R. Kenigsberg[19], Mebae Kuranaga[20], Steffen Kutterolf[21], Freya L. Mitchison[22], Hideki Mukoyoshi[23], Nisha Nair[24], Kevin T. Pickering[25], Hugo F.A. Pouderoux[26], Yehua Shan[11], Insun Song[27] Paola Vannucchi[28], Peter J. Vrolijk[29], Tao Yang[30], Xixi Zhao[31]

*corresponding author: ahuepers@uni-bremen.de

Affiliations:

[1]MARUM-Center for Marine Environmental Sciences, University of Bremen, PO Box 330 440, D-28334 Bremen, Germany, ahuepers@uni-bremen.de, Tel: (49) 421-21865-814

[2]College of Earth, Ocean and Atmospheric Sciences, Oregon State University, 104 CEOAS Admin Building, Corvallis OR 97331-5503, USA

[3]Department of Earth Sciences, Chiba University, 1-33 Yayoi-cho, Inage-ku, Chiba City 263-8522, Japan

[4]Ocean and Earth Science, National Oceanography Centre Southampton, University of Southampton, Southampton S014 3ZH, United Kingdom

[5]Department of Geophysics, Colorado School of Mines, Golden CO 80401, USA

[6]Bureau of Economic Geology, 1 University Station, Box X, Austin TX 78713, USA

[7]International Ocean Discovery Program, Texas A&M University, 1000 Discovery Drive, College Station TX 77845, USA

[8]Department of Geological Sciences, Stockholm University, SE-106 91 Stockholm, Sweden

[9]Laboratoire GeoRessources, CNRS-Université de Lorraine-CREGU, Ecole Nationale Supérieure de Géologie, Rue du Doyen Marcel Roubault, TSA 70605 – 54518, Vandoeuvre-lès-Nancy, France

[10]Programa de Pós-Graduação em Geologia, Universidade do Vale do Rio dos Sinos,

93.022-000 São Leopoldo - RS Brasil, Brazil

[11]Key Laboratory of Marginal Sea Geology , Chinese Academy of Sciences, #511 Kehua Street, Tianhe District, Guangzhou 510640, P.R. China

[12]School of Earth Sciences, University of Western Australia, 35 Stirling Highway, Crawley 6009, Australia

[13]Center for Regional Resources Development Technology (PTPSW-TPSA), Agency for the Assessment and Application of Technology (BPPT), Bldg. 820, Earth System Technology (Geostech), Kawasan Puspitek Serpong, South Tangerang, Banten, Indonesia 15314, Indonesia

[14]Lamont-Doherty Earth Observatory, Columbia University, Borehole Research Group, 61 Route 9W, Palisades NY 10964, USA

[15]Geophysics Research Group, Institute of Geology and Geoinformation, Geological Survey of Japan (AIST), AIST Tsukuba Central 7, 1-1-1 Higashi, Tsukuba Ibaraki 305-8567, Japan

[16]Scripps Institution of Oceanography, University of California, San Diego, Vaughan Hall 434, 8675 Discovery Way, La Jolla, CA 92037, USA

[17]Department of Geology and Geophysics, University of Wisconsin-Madison, 1215 W. Dayton Street, Madison WI 53706, USA

[18]Department of Geography Planning and Environmental Management, Level 4, Building 35, The University of Queensland, Brisbane, QLD, Australia

[19]Department of Geosciences, Pennsylvania State University, 503 Deike Building, University Park PA 16802, USA

[20]Graduate School of Science and Engineering, Yamaguchi University, 1677-1 Yoshida

Yamaguchi City 753-8512, Japan

[21]GEOMAR, Helmholtz Center for Ocean Research Kiel, Wischhofstr. 1-3, Kiel 24148, Germany

[22]School of Earth and Ocean Sciences, Cardiff University, Park Place, Cardiff CF10 3XQ, United Kingdom

[23]Department of Geoscience, Shimane University, 1060 Nishikawatsu-cho, Matsue, Shimane 690-8504, Japan

[24]CLCS/Marine Geophysical Division, National Centre for Antarctic and Ocean Research, Earth System Science Organization, Ministry of Earth Sciences, Government of India, Headland Sada, Vasco-da-Gama, Goa – 403804, India

[25]Earth Sciences, University College London, London WC1E 6BT, United Kingdom

[26]CNRS, UMR6118 - Geosciences Rennes, University de Rennes I, Campus de Beaulieu,

35042 Rennes Cedex, France

[27]Geologic Environmental Division, Korea Institute of Geoscience & Mineral (KIGAM), 124 Gwahak-ro, Yuseong-gu, Daejeon 34132, Korea

[28]Royal Holloway and Bedford New College, Royal Holloway University of London, Queens Building, Egham TW20 0EX, United Kingdom

[29]New Mexico Tech, 801 Leroy Place, Socorro, NM 87801, USA

[30]Institute of Geophysics, China Earthquake Administration, #5 Minzu Daxue Nanlu, Hiadian District, Beijing 100081, P.R. China

[31]Department of Earth and Planetary Sciences, University of California, Santa Cruz, 1156 High Street, Santa Cruz CA 95064, USA

Abstract:

Plate-boundary fault rupture during the 2004 Sumatra-Andaman subduction earthquake extended closer to the trench than expected, increasing earthquake and tsunami size. International Ocean Discovery Program Expedition 362 sampled incoming sediments offshore Northern Sumatra, revealing recent release of fresh water within the deep sediments. Thermal modeling links this freshening to amorphous silica dehydration driven by rapid burial-induced temperature increases in the last 9 Myr. Complete dehydration of silicates is expected before plate subduction, contrasting with prevailing models for subduction seismogenesis calling for fluid production during subduction. Shallow slip offshore Sumatra appears driven by diagenetic strengthening of deeply buried fault-forming sediments, contrasting with weakening proposed for the shallow Tohoku-oki 2011 rupture, but our results are applicable to other thickly-sedimented subduction zones including those with limited earthquake records.

One Sentence Summary:

Dehydration of buried silicates within Sumatra input sediments before subduction explains shallow slip of the 2004 M_W≈9.2 earthquake.

Main Text:

The largest earthquakes occur along subduction plate boundary faults and typically generate large, far-reaching tsunamis. The mechanical (e.g, unstable sliding rheology) and hydrogeological conditions (i.e., fluid generation) of the fault interface, which depend on the properties of the materials being subducted, control where and when megathrust earthquakes occur as well as the earthquake magnitude and tsunami hazard (*1*, *2*). Current models tie the updip limit of seismogenesis, and hence the seaward extent and width of the earthquake rupture, to mechanical compaction and mineral dehydration reactions that generate fluids and promote lithification within the subduction zone (landward of the deformation front) (*2*, *3*). These models lead to predictions that rupture should occur at depth within the subduction zone with limited coseismic slip in the outer forearc (*2*, *4*). However, during the 2004 Sumatra-Andaman and the 2011 Tohoku-Oki earthquakes, slip extended much farther and closer to the seaward limits of the subduction forearc than predicted (*5*), resulting in wider rupture zones, larger earthquakes, and tsunamis.

This unexpected behavior requires reappraisal of models of subduction earthquake seismogenesis and a better understanding of the sediments that form megathrust faults, ultimately through direct sampling of fault or fault-forming materials.

On 26 December 2004, a M_W≈9.2 earthquake ruptured ~1300 km from offshore northern Sumatra to the Andaman Islands, where the Indo-Australian plate subducts beneath the Burma-Sunda plate (*6*; Fig. 1), causing the devastating tsunami that killed more than 250,000 people (*7*). Coseismic slip propagated seaward beneath the accretionary prism, possibly extending to the trench (*8, 9*). Previously, the outermost plate-boundary fault (or décollement) at subduction zones had been assumed to be primarily aseismic (*2, 4*) so that the main seismic moment release was expected farther landward, as observed during the 2005 M_W≈8.7 Nias earthquake offshore Central Sumatra (*10*, Fig. 1) and at other accretionary margins (*2, 4*). Seismic slip models (*11, 12*) show that rupture nucleation and propagation of the 2004 earthquake offshore northern Sumatra occurred largely under a broad plateau in the accretionary prism. Previous studies (*13*-*15*) related this to strengthening of the incoming sediment outboard of the subduction zone, leading to a seaward shift of seismogenesis.

The Sumatra margin is distinctive from other accretionary margins because the incoming sequence is up to 4-5 km thick at the deformation front and includes thick sediments of the Bengal-Nicobar fan. It is also characterized by a seismic horizon that develops into a high amplitude negative polarity (HANP) seismic reflector near the subduction zone (*13*, Fig. 1). The HANP horizon has been interpreted as a weak, porous, overpressured, fluid-rich layer that is the locus for décollement initiation along parts of the margin, based on fault interpretation of seismic data (*13*). During International Ocean Discovery Program (IODP) Expedition 362 we sampled sediments about ~225 km seaward of the North Sumatran deformation front, including the sediments that ultimately form the Sunda plate boundary fault and forearc. At Site U1480, we recovered input sediment to basement at ~1420 mbsf (meters below seafloor) and we sampled sediment at Site U1481 from 1150 to 1500 mbsf (Fig. 1, Fig. S1). The thick sedimentary sequence reflects the >200 m/Myr Nicobar fan deposition that began ~9 Myr ago (units I and II, Fig. 2, *16*). On approaching the subduction zone, the plate flexes and rapid sedimentation adds an additional

~2-3 km of trench wedge sediment to the input sequence (Fig. 1b). Geochemical analyses show that sediment in the volcanogenic-rich pelagic unit underlying the Nicobar Fan sequence (unit III, Fig. S1) contains >20 wt.-% amorphous silica (*16*-*18*), which constitutes a significant reservoir of mineral-bound water available for release upon dehydration (Fig. 2). Smear slide observations of samples from this unit document the presence of dominantly clay-size, amorphous and poorly crystalline silicate material, identified as palagonite, with minor fragmented sponge spicules and radiolaria (Fig. S2). X-ray diffraction analyses (XRD, Fig. S3) support geochemical and smear slide inferences for the presence of amorphous and poorly crystalline silicates. These amorphous silicates reflect complete alteration and hydration of volcanic glass, which we attribute to ~30 Myr of seawater exposure during the slow accumulation of the pelagic sediment (Fig. 2). We also found evidence of recent dehydration reactions of these altered sediments within unit III as documented by a sharp, ~80-m thick freshening anomaly, where chloride decreases from ~580 mM to ~520 mM (U1480: 1250-1330 mbsf, U1481: 1350-1450 mbsf) and interpret this as a response to rapid Nicobar Fan sedimentation (Fig. 2, Fig. S4, *16*). We used a simple diffusion model to show that this freshening occurred very recently (last 100 kyr) (*17*) (Fig. S4). The same stratigraphic interval in unit III corresponds to increased porosity (Fig. S5) and is correlated to the HANP seismic horizon (*13*, Fig. 1).

To mechanistically test what drives shallow seismogenesis and to elucidate the origin of the HANP reflector, we modeled fluid production of the incoming sediment using reaction kinetics (*19*, *20*) along a time-temperature progression of unit III sediments from deposition to accretion at the subduction zone (*17*, Fig. S6). Our models predict most of the observed freshening at the drilled sites can be explained by biosilica dehydration (Fig. 3) as the pelagic sediments reached >50°C <1 Myr, facilitating the transition from opal-A to opal-CT to quartz (Fig. 3). The observed freshening corresponds to a biosilica input of ~18 wt.-%, which falls within the range expected for Eocene pelagic sediments (*18*). The calculated reaction progress suggests 4 wt.-% opal-A, 2 wt.-% opal-CT and 12 wt.-% quartz at the present location of Site U1480, consistent with XRD data. We projected the dehydration simulations to estimate fluid production as temperature increases towards the subduction deformation front. Given uncertainties regarding palagonite dehydration kinetics (*21*), we used smectite as a palagonite proxy to model the altered volcanogenic component undergoing dehydration, consistent with our XRD results showing a poorly crystalline expandable clay as the dominant material in the palagonite and that smectite is the final replacement product of palagonitization (*21*). Model results (Fig. 3) demonstrate that fluid production from opal dehydration peaks before sediments enter the trench, smectite/palagonite dehydration peaks close to the deformation front, and that fluids produced by dehydration reactions exceed fluids produced by compaction-driven dewatering (Fig. 3). We acknowledge uncertainties in these estimates, which include: a) the opal water content, which we assumed to be 12.1 wt-% (*22*); b) the onset of palagonite dehydration, which we assumed to follow smectite kinetics (*19*); and c) the depth estimate of unit III in the trench. A lower amount of water-bound opal and an earlier onset of palagonite dehydration dehydration (relative to the onset expected from the smectite proxy) may balance to account for the freshening observed at Site U1480. We note that in addition to palagonite, smectite itself may also contribute to fluid production pre-subduction. Water released from smectite/palagonite corresponding to sediment loading at the trench is indicated in Fig. 3. Notwithstanding the uncertainties, our simulations show that dehydration leads to pre-subduction pore fluid production that is consistent with the HANP reflector observable seaward of the North Sumatra trench (Fig. 1), and point to a larger pore fluid content in this area relative to Central Sumatra (Fig. 1, *13*). The lack of strong décollement reflectivity beneath the prism (*13)* further supports that, by this stage, either dehydration is minimal and/or produced fluids are rapidly released from the décollement.

The level of compaction and diagenesis of the incoming sediment to North Sumatra differs from that of well-studied accretionary margins such as Nankai or northern Barbados Ridge (Lesser Antilles). At the level of the décollement, compaction and diagenesis are more limited by the trench and outermost forearc at Nankai and Barbados (from drilling results) than modeled for North Sumatra (see Table S1, *17*), including the Nankai-Muroto transect where high heat flow leads to shallow and early diagenesis (see Table S1). Hydrogeological models of these margins showed that excess pore pressures from porosity reduction and mineral dehydration dissipate from the décollement horizon at or near the updip limit of seismogenesis, deeper within the subduction zone and not in the outermost forearc (*2*, *3*). Burial by thick Nicobar Fan and trench wedge sediments offshore North Sumatra causes mechanical compaction and mineral dehydration along the proto-décollement to reach completion before subduction (Fig. 3). Early diagenesis creates a fluid pressure pulse that dissipates from the décollement horizon within the outermost forearc, as evidenced by the seismically reflective outer prism faults and by a reduction in reflection amplitude at the HANP horizon beneath the toe of the prism (*13, 14*). The increase in effective stress from the pressure dissipation and the precipitation of quartz from opal diagenesis (*23*) and smectite-to-illite transformation (*3*) are consistent with a tendency towards an unstable sliding rheology (*3*, *24*) that extends seismogenesis seaward to the shallow outer forearc.

Sampling of the fault-forming materials at the North Sumatran subduction zone provides direct evidence that diagenesis before subduction may drive shallow slip and therefore the unexpected increase in earthquake rupture width and magnitude. The Sumatra-Andaman 2004 and Tohoku-Oki 2011 earthquakes both had shallow slip, but with different driving processes. Both events show that the commonly accepted seismogenic model of nucleation deep within the subduction zone and limited seaward rupture is just one among a varied set of conditions that control earthquake rupture and coseismic slip. The shallow slip along the Japan Trench was attributed to a weak, smectite-rich fault zone (*25*) while shallow slip offshore North Sumatra occurred on a clay-rich fault that was strengthened by diagenesis. The model derived from our analysis of the Sumatran core samples may be applicable to other subduction zones that have thick input sediments or high temperatures or both, including the Makran, Cascadia, southern Lesser Antilles, and Eastern Aleutians (*25;* Table S1). The thickness and thermal state of sediments at the Cascadia, southern Lesser Antilles, and Makran margins (Table S1), all affected by input of submarine fan sequences, suggest similarities to North Sumatra in terms of state of diagenesis and potential for shallow slip. We also note that although dehydration is modeled to peak within and not outboard of the Eastern Aleutians subduction zone (*26*), slip in the outermost forearc was recorded during the 1964 earthquake (*27*) (Table S1). Many of these subduction zones have either never been sampled (e.g., Makran) or have a limited historic rupture record (e.g., Makran, southern Lesser Antilles, Cascadia), but shallow slip during megathrust rupture may be possible. As the specific earthquake and tsunami potential is not well known in these regions, a wide range of models should be applied to better assess the range of earthquake magnitude and tsunamigenesis possible from a large megathrust earthquake.

References and Notes:

1 M. B. Underwood. “Sediment inputs to subduction zones” in *The Seismogenic Zone of Subduction Thrust Faults*, T. H. Dixon J. C. Moore, Eds. (Columbia Univ. Press, NY, 2007).

2 D. M. Saffer, H. J. Tobin, Hydrogeology and mechanics of subduction zone forearcs: fluid flow and pore pressure. *Annu. Rev. Earth Pl. Sc.* ***39***, 157–186 (2011).

3 J. C. Moore, D. M. Saffer, Updip limit of the seismogenic zone beneath the accretionary prism of southwest Japan: An effect of diagenetic to low-grade metamorphic processes and increasing effective stress, *Geology* ***29***, 183-186 (2001).

4 K. Wang, Y. Hu, Accretionary prisms in subduction earthquake cycles: The theory of dynamic Coulomb wedge. *J. Geophys. Res.* ***111***, B06410, (2006).

5 M. Simons, S. E. Minson, A. Sladen, F. Ortega, J. Jiang, S. E. Owen, S. E, L. Meng, J. P. Ampuero, S. Wei, R. Chu, D. V. Helmberger, H. Kanamori, E. Hetland, A. W. Moore, F. H. Webb, The 2011 magnitude 9.0 Tohoku-Oki earthquake: Mosaicking the megathrust from seconds to centuries. *Science* ***332***, 1421-1425 (2011).

6 W. J. F. Simons, A. Socquet, C. Vigny, B. A. C. Ambrosius, S. Haji Abu, C. Promthong, D. A. Sarsito, S. Matheussen, P. Morgan, W. Spakman, A decade of GPS in Southeast Asia: Resolving Sundaland motion and boundaries. *J. Geophys. Res.-Sol. Ea.* ***112*** (2007).

7 T. Lay, H. Kanamori, C. J. Ammon, M. Nettles, S. N. Ward, R. C. Aster, S. L. Beck, S. L. Bilek, M. R. Brudzinski, R. Butler, H. R. DeShon, G. Ekström, K. Satake, S. Sipkin, The great Sumatra-Andaman earthquake of 26 december 2004. *Science* ***308***, 1127-1133 (2005).

8 T. J. Henstock, L. C. McNeill, D. R. Tappin, Seafloor morphology of the Sumatran subduction zone: Surface rupture during megathrust earthquakes ?. *Geology* ***34***, 485–488 (2006).

9 Q. Bletery, A. Sladen, J. Jiang, M. Simons, A Bayesian source model for the 2004 great Sumatra-Andaman earthquake. *J. Geophys. Res.-Sol. Ea.* ***121***, 5116-5135 (2016).

10 R. W. Briggs, K. Sieh, A. J. Meltzner, D. Natawidjaja, J. Galetzka, B. Suwargadi, Y. Hsu, M. Simons, N. Hananto, I.Suprihanto, D. Prayudi, J.-P.Avouac, L. Prawirodirdjo, Y. Bock, Deformation and slip along the Sunda megathrust in the great 2005 Nias-Simeulue earthquake. *Science* ***311***, 1897-1901 (2006).

11 J. Rhie, D. Dreger, R. Bürgmann, B. Romanowicz, Slip of the 2004 Sumatra–Andaman earthquake from joint inversion of long-period global seismic waveforms and GPS static offsets. *Bull. Seismol. Soc. Am.* ***97***, 115-127 (2007).

12 Y. Fujii, K. Satake, K., Tsunami source of the 2004 Sumatra–Andaman earthquake inferred from tide gauge and satellite data. *B. Seismol. Soc. Am.* ***97***, 192-207 (2007).

13 S. M. Dean, L. C. McNeill, T. J. Henstock, J. M. Bull, J. M., S. P. Gulick, J. A. Austin, J. A., N. L. Bangs, Y. S. Djajadihardja, H. Permana, Contrasting décollement and prism properties over the Sumatra 2004–2005 earthquake rupture boundary. *Science* ***329***, 207-210 (2010).

14 S. P. Gulick, J. A. Austin, L. C. McNeill, N. L. Bangs, K. M. Martin, T. J. Henstock, J. M. Bull, S. Dean, Y. S. Djajadihardja, H. Permana, Updip rupture of the 2004 Sumatra earthquake extended by thick indurated sediments. *Nat. Geosci.* ***4***, 453-456 (2011).

15 J. Geersen, D. J. Wilson, B. Cook ,L. C. McNeill, T. J. Henstock, C. Gaedicke, C., The 2004 Aceh-Andaman Earthquake: Early clay dehydration controls shallow seismic rupture. *Geochem. Geophys. Geosys.* ***14***, 3315-3323 (2013).

16 B. Dugan, L. C. McNeill, K. Petronotis and the Expedition 362 Scientists, *Expedition 362 Preliminary Report: Sumatra Subduction Zone - The role of input materials in shallow seismogenic slip and forearc plateau development.* (International Ocean Discovery Program, http://dx.doi.org/10.14379/iodp.pr.362.2017, 2017).

17 Materials and methods are available as supporting material on Science Online.

18 A. O. Lyle, M. W. Lyle, “Determination of biogenic opal in pelagic marine sediments: a simple method revisited” in *Proc. ODP. Init. Repts. 199*, M. Lyle, P. A. Wilson, T. R. Janecek, et al., Eds. (College Station, TX (Ocean Drilling Program), 2002).

19 W. L. Huang, J. M. Longo, D. R. Pevear, An experimentally derived kinetic model for smectite-to-illite conversion and its use as a geothermometer. *Clays Clay Min.* ***41***, 162-162 (1993).

20 S. Mizutani, Silica minerals in the early stage of diagenesis. *Sedimentology* ***15***, 419–436 (1970).

21 N. A. Stroncik, H. U. Schmincke, Palagonite–a review. *Int. J. Earth Sci.* ***91***, 680-697 (2001).

22 R. Day, B. Jones, Variations in water content in opal-A to opal-CT from geyser discharge aprons, *J. Sediment. Res.* **78**, 301–315 (2008).

23 K. Bjorlykke, P. K. Egeberg, Quartz cementation in sedimentary basins. *AAPG Bull.* ***77***, 1538-1548 (1993).

24 S. Trütner, A. Hüpers, M. J. Ikari, A. Yamaguchi, A. J. Kopf, Lithification facilitates frictional instability in argillaceous subduction zone sediments. *Tectonophysics* ***665***, 177–185 (2015).

25 K. Ujiie, H. Tanaka, T. Saito, A. Tsutsumi, J. Mori, J. Kameda, E. E. Brodsky, F. M. Chester, N. Eguchi, S. Toczko, and Expedition 343 and 343T Scientists, Low coseismic shear stress on the Tohoku-Oki megathrust determined from laboratory experiments. *Science* ***342***, 1211-1214 (2013).

26 G. L. Smith, L. C. McNeill, K. Wang, J. He, T. J. Henstock, Thermal structure and megathrust seismogenic potential of the Makran subduction zone. *Geophys. Res. Lett.* ***40***, 1528-1533 (2013).

27 L. N. Meridth, E. J. Screaton, J. M. Jaeger, S. R. James, T. Villasenor, The impact of rapid sediment accumulation on pore pressure development and dehydration reactions during shallow subduction in the Gulf of Alaska. *Geochem. Geophys. Geosyst.* ***18***, 189 - 203, doi:10.1002/2016GC006693 (2017).

28 G. Ichinose, P. Somerville, H. K. Thio, R. Graves, D. O’Connell, Rupture process of the 1964 Prince William Sound, Alaska, earthquake from the combined inversion of seismic, tsunami, and geodetic data. *J. Geophys. Res.* ***112***, B07306, doi:10.1029/2006JB004728 (2007).

Figure captions

29 A. J. Meltzner, K. Sieh, H.-W. Chiang, C.-C. Shen, B. W. Suwargadi, D. H. Natawidjaja, B. Philibosian, R. W. Briggs, Persistent termini of 2004- and 2005-like ruptures of the Sunda megathrust. *J. Geophys. Res.-Sol. Ea.* ***117***, B04405 (2012).

30 L. C. McNeill, T. J. Henstock, Forearc structure and morphology along the Sumatra-Andaman subduction zone. *Tectonics* ***33***, 112-134 (2014).

31 S. C. Singh, N. D. Hananto, A. P. Chauhan, Enhanced reflectivity of backthrusts in the recent great Sumatran earthquake rupture zones. *Geophys. Res. Lett.* ***38***, *L04302* (2011).

Methods

32 F. T. Manheim, A hydraulic squeezer for obtaining interstitial waters from consolidated and unconsolidated sediments, *Geol. Surv. Prof. Pap. U.S.* ***550-C***, 256-261 (1966).

33 T. G. Fitts, K. M. Brown, Stress-induced smectite dehydration: Ramifications for patterns of freshening and fluid expulsion in the N. Barbados accretionary wedge, *Earth Planet. Sci. Lett.* **172**, 179–197, doi:10.1016/S0012-821X(99)00168-5 (1999).

34 K. Grasshoff, K. Kremling, M. Ehrhardt, M. Methods of Sea water Analysis. (Wiley, NY, 1999).

35 R. A. Berner, Early Diagenesis: A Theoretical Approach (Princeton Univ. Press, Princeton, NJ, 1980).

36 B. P. Boudreau, Diagenetic Models and Their Implementation: Modelling Transport and Reactions in Aquatic Sediments (Springer, Berlin, 1997).

37 M. K. Hubbert, W. W. Rubey, Role of fluid pressure in mechanics of overthrust faulting I. Mechanics of fluid-filled porous solids and its application to overthrust faulting. *Geol. Soc. Am. Bull.* ***70***, 115-166 (1959).

38 E. C. Bullard, Heat flow in South Africa. *Proc. R. Soc. London Ser. A* ***173***, 474–502 (1939).

39 B. Parsons, J. G. Sclater, J. G. An analysis of the variation of ocean floor bathymetry and heat flow with age. *J Geophys Res.* ***82***, 803-827 (1977).

40 C. A. Stein, S. Stein, A model for the global variation in oceanic depth and heat flow with lithospheric age. *Nature* ***359***, 123-129 (1992).

41 J. Jacob, J. Dyment, V. Yatheesh, Revisiting the structure, age, and evolution of the Wharton Basin to better understand subduction under Indonesia. *J. Geophys. Res.-Sol. Ea.* ***119***, 169-190 (2014).

42 D. M. Saffer, M. B. Underwood, A. W. McKiernan, Evaluation of factors controlling smectite transformation and fluid production in subduction zones: application to the Nankai Trough. *Isl. Arc* ***17***, 208-230 (2008).

43 G. Kimura, S. Hina, Y. Hamada, J. Kameda, T. Tsuji, M. Kinoshita, A. Yamaguchi, Runaway slip to the trench due to rupture of highly pressurized megathrust beneath the middle trench slope: The tsunamigenesis of the 2011 Tohoku earthquake off the east coast of northern Japan, *Earth Planet. Sci. Lett.* **339**, 32–45 (2012).

44 G. A. Spinelli, M. B. Underwood, Character of sediments entering the Costa Rica subduction zone: Implications for partitioning of water along the plate interface. *Isl. Arc* ***13***, 432-451 (2004).

45 A. Taira, I. Hill, J.V. Firth, et al., Proc. ODP. *Init. Repts. 131* (College Station, TX (Ocean Drilling Program), doi:10.2973/odp.proc.ir.131.1991, 1991).

46 G. F. Moore, A. Taira, A. Klaus, et al., *Proc. ODP. Init. Repts. 190* (College Station, TX (Ocean Drilling Program), doi:10.2973/odp.proc.ir.190.2001, 2001).

47 R. Harris, M. Yamano, M. Kinoshita, G. A. Spinelli, H. Hamamoto, J. and Ashi, A synthesis of heat flow determinations and thermal modeling along the Nankai Trough, Japan. *J. Geophys. Res.* ***118***, 2687-2702 (2013).

48 G. A. Spinelli, K. Wang, Effects of fluid circulation in subducting crust on Nankai margin seismogenic zone temperatures. *Geology* ***36***, 887–890 (2008).

49 R. D. Hyndman, K. Wang, M. Yamano, Thermal constraints on the seismogenic portion of the southwestern Japan subduction thrust. *J. Geophys. Res.* ***100***, 15,373–15,392 (1995).

50 J. F. Steurer, M. B. Underwood, “Clay mineralogy of the Nankai Trough accretionary prism and reference sites” in *Proc. ODP*, *Sci. Res. 190/196*, H. Mikada G. F. Moore, A. Taira, K. Becker, J. C. Moore, A. Klaus, Eds. (College Station, TX (Ocean Drilling Program), 2003).

51 M. Kinoshita, H. Tobin, J. Ashi, G. Kimura, S. Lallemant, E.J. Screaton, D. Curewitz, H. Masago, K.T. Moe, and the Expedition 314/315/316 Scientists, *Proc. IODP 314/315/316* (Washington, DC (Integrated Ocean Drilling Program Management International, Inc.), doi:10.2204/ iodp.proc.314315316.2009, 2009).

52 S. Saito, M. B. Underwood, Y. Kubo, and the Expedition 322 Scientists, *Proc. IODP* 322. (Tokyo (Integrated Ocean Drilling Program Management International, Inc.), doi:10.2204/iodp.proc.322.2010, 2010).

53 M. B. Underwood, J. Guo, “Data report: clay mineral assemblages in the Shikoku Basin, NanTroSEIZE subduction inputs, IODP Sites C0011 and C0012” in *Proc. IODP 322*, S. Saito, M.B. Underwood, Y. Kubo, and the Expedition 322 Scientists, Eds. (Tokyo (Integrated Ocean Drilling Program Management International, Inc.), doi:10.2204/iodp.proc.322.202.2013, 2013).

54 G. A. Spinelli, R. N. Harris, Thermal effects of hydrothermal circulation and seamount subduction: Temperatures in the Nankai Trough Seismogenic Zone Experiment transect, Japan. *Geochem. Geophys. Geosyst.* ***12***, Q0AD21, doi:10.1029/2011GC003727 (2011).

55 G.F. Moore, J.-O. Park, N. L. Bangs, S. P. Gulick, H. J. Tobin, Y. Nakamura, S. Sato, T. Tsuji, T. Yoro, H. Tanaka, S. Uraki, Y. Kido, Y. Sanada, S. Kuramoto, A. Taira, “Structural and seismic stratigraphic framework of the NanTroSEIZE Stage 1 transect” in *Proc. IODP 314/315/316***,** M. Kinoshita, H. Tobin, J. Ashi, G. Kimura, S. Lallement, E. J. Screaton, D. Curewitz, H. Masago, K. T. Moe and the Expedition 314/315/316 Scientists (Washington, DC (Integrated Ocean Drilling Program Management International, Inc.), doi:10.2204/iodp.proc.314315316.102.2009, 2009).

56 L. D. Kulm, R. von Huene, et al., *Init. Repts. DSDP 18* (Washington, D.C., U.S. Government Printing Office, 1973).

57 E. E. Davis, A. T. Fisher, J. V Firth, et al., *Proc. ODP. Init. Repts. 168* (College Station, TX (Ocean Drilling Program). doi:10.2973/odp.proc.ir.168.1997, 1997).

58 M. B. Underwood, Strike-parallel variations in clay minerals and fault vergence in the Cascadia subduction zone. *Geology* ***30***, 155-158 (2002).

59 R. D. Hyndman, K. Wang, The rupture zone of Cascadia great earth- quakes from current deformation and the thermal regime. *J. Geophys. Res.* ***100***, 22,133–22,154 (1995).

60 G. Booth- Rea, D. Klaeschen, I. Grevemeyer, T. Reston, Heterogeneous deformation in the Cascadia convergent margin and its relation to thermal gradient (Washington, NW USA). *Tectonics* ***27***, TC4005, doi:10.1029/2007TC002209 (2008).

61 A. Mascle, J. C. Moore, et al., *Proc. ODP. Init. Repts. 110* (College Station, TX (Ocean Drilling Program). doi:10.2973/odp.proc.ir.110.1988, 1988).

62 T. H. Shipley, Y. Ogawa, P. Blum, et al., *Proc. ODP. Init. Repts. 156* (College Station, TX (Ocean Drilling Program). doi:10.2973/odp.proc.ir.156.1995, 1995).

63 J. C. Moore, A. Klaus, et al., *Proc. ODP. Init. Repts. 171A* (College Station, TX (Ocean Drilling Program). doi:10.2973/odp.proc.ir.171a.1998, 1998).

64 N. L. B. Bangs, G.K. Westbrook, J.W. Ladd, P. Buhl, Seismic velocities from the Barbados Ridge Complex: Indicators of high pore-fluid pressure in an accretionary complex. *J. Geophys. Res.* ***95***, 8767-8782 (1990).

65 N. L. B. Bangs, T. H. Shipley, J. C. Moore, G. F. Moore, Fluid accumulation and channeling along the northern Barbados Ridge decollement thrust. *J. Geophys. Res.* ***104***, 20399-20414 (1999).

66 G. K. Westbrook, M. J. Smith, Long decollements and mud volcanoes: evidence from the Barbados Ridge complex for the role of high pore fluid pressure in the development of an accretionary complex. *Geology* ***11***, 279–283 (1983).

67 G. K. Westbrook, G.K., A. Mascle, and B. Biju-Duval, “Geophysics and the structure of the Lesser Antilles forearc” in *Init. Repts. DSDP 78A*, B. Biju-Duval, J. C. Moore, et al., Eds. (Washington (U.S. Govt. Printing Office). doi:10.2973/dsdp.proc.78a.102.1984, 1984).

68 J. S. Tribble, “Clay diagenesis in the Barbados accretionary complex: potential impact on hydrology and subduction dynamics” in *Proc. ODP. Sci. Res. 110*, J. C. Moore, A. Mascle, et al., Eds. (College

Station, TX (Ocean Drilling Program), 97–110. doi:10.2973/odp.proc.sr.110.131.1990, 1990).

69 A. T. Fisher, M. W. Hounslow, "Heat flow through the toe of the Barbados accretionary complex" in *Proc. ODP. Sci. Results 110*, J. C. Moore, A. Mascle, et al., Eds. (College Station, TX (Ocean Drilling Program), doi:10.2973/odp.proc.sr.110.154.1990, 1990).

70 M.-A. Gutscher, G. K. Westbrook, B. Marcaillou, D. Graindorge, A. Gailler, T. Pichot, R. C. Maury, How wide is the seismogenic zone of the Lesser Antilles forearc?. *Bull. Soc. Geol. France* ***184***, 47-59 (2013).

71 B. A. Bekins, A. M. McCaffrey, S. J. Dreiss, Influence of kinetics on the smectite to illite transition in the Barbados accretionary prism. *J. Geophys. Res.-Sol.Ea.* ***99***, 18147-18158 (1994).

72 G. Smith, L. C. McNeill., T. J. Henstock, J. Bull, The structure and fault activity of the Makran accretionary prism. *J. Geophys. Res.* ***117***, B07407, doi:10.1029/2012JB009312 (2012).

73 V. Vacquier, P. T. Taylor, Geothermal and magnetic survey off the coast of Sumatra–1. Presentation of data. *B Earthq. Res. I. Tokyo* ***44***, 531–540 (1966).

74 F. Klingelhoefer, M.-A. Gutscher, S. Ladage, J.-X. Dessa, D. Graindorge, D. Franke, C. André, H. Permana, T. Yudistira, A. Chauhan,Limits of the seismogenic zone in the epicentral region of the 26 December 2004 great Sumatra-Andaman earthquake: results from seismic refraction and wide-angle reflection surveys and thermal modeling. *J. Geophys. Res.* ***115(B1)***, B01304, dx.doi.org/10.1029/2009JB006569 (2010).

75 L. D. Kulm, R. von Huene, et al., *Init. Repts. DSDP 18* (Washington, DC (U.S. Govt. Printing Office), doi:10.2973/dsdp.proc.18.1973, 1973).

76 J. M. Jaeger, S. P. S. Gulick, L. J. LeVay, L.J., and the Expedition 341 Scientists, *Proc. IODP 341* (College Station, TX (Integrated Ocean Drilling Program), doi:10.2204/iodp.proc.341.2014, 2014).

77 R. S. Reece, S. P. S. Gulick, B. K. Horton, G. L. Christeson, L. L. Worthington, Tectonic and climatic influence on the evolution of the Surveyor Fan and Channel system, Gulf of Alaska. *Geosphere* ***7***, 830–844, doi:10.1130/GES00654.1 (2011).

78 M. C. G. Frederik, Morphology and structure of the accretionary prism offshore North Sumatra,

Indonesia and offshore Kodiak Island, USA: A comparison to seek a link between prism formation and hazard potential (PhD thesis, Univ. of Texas at Austin, Austin, 2016).

79 G. Kimura, E. A. Silver, P. Blum, et al., *Proc. ODP. Init. Repts. 170* (College Station, TX (Ocean Drilling Program). doi:10.2973/odp.proc.ir.170.1997, 1997).

80 J. D. Morris, H. W. Villinger, A. Klaus, et al., *Proc. ODP. Init. Repts. 205* (College Station, TX (Ocean Drilling Program). doi:10.2973/odp.proc.ir.205.2003, 2003).

81 P. Vannucchi, K. Ujiie, N. Stroncik, and the Expedition 334 Scientists, *Proc. IODP 334* (Tokyo (Integrated Ocean Drilling Program Management International, Inc.). doi:10.2204/iodp.proc.334.2012, 2012).

82 R. N. Harris, G. A. Spinelli, C. R. Ranero, I. Grevemeyer, H. Villinger, U. Barckhausen, Thermal regime of the Costa Rican convergent margin: 2. Thermal models of the shallow Middle America subduction zone offshore Costa Rica. *Geochem. Geophys. Geosyst.* ***11***, Q12S29, doi:10.1029/2010GC003273 (2010).

83 R. N. Harris, A. Sakaguchi, K. Petronotis, K., and the Expedition 344 Scientists, *Proc. IODP 344* (College Station, TX (Integrated Ocean Drilling Program). doi:10.2204/iodp.proc.344.2013, 2013).

84 G. A. Spinelli, D. M. Saffer, Along-strike variations in underthrust sediment dewatering on the Nicoya margin, Costa Rica related to the updip limit of seismicity. *Geophys. Res. Lett.* ***31***, L04613, doi:10.1029/2003GL018863 (2004).

85 N. L. B. Bangs, , K. D. McIntosh, E. A. Silver, J. W. Kluesner, C. R. Ranero, Fluid accumulation along the Costa Rica subduction thrust and development of the seismogenic zone. *J. Geophys. Res.* ***120***, 67–86, doi:10.1002/2014JB011265 (2015).

86 F. M. Chester, J. Mori, N. Eguchi, S. Toczko, and the Expedition 343/343T Scientists, *Proc. IODP 343/343T*, (Tokyo (Integrated Ocean Drilling Program Management International, Inc.). doi:10.2204/iodp.proc.343343T.2013, 2013).

87 F.M. Chester, et al. Structure and Composition of the Plate-Boundary Slip Zone for the 2011 Tohoku-Oki Earthquake. *Science* ***342***, 1208-1211, doi:10.1126/science.1243719 (2013).

88 S. Kodaira, T. No, Y. Nakamura, T. Fujiwara, Y. Kaiho, N. Takahashi, Y. Kaneda, A. Taira, Coseismic fault rupture at the trench axis during the 2011 Tohoku-oki earth-quake. *Nat. Geosci.* ***5***, 646–650, doi:10.1038/ngeo1547 (2012).

89 P. M. Fulton, E. E. Brodsky, Y. Kano, J. Mori, F. M. Chester, T. Ishikawa, R. N. Harris, W. Lin, N. Eguchi, S. Toczko, and Expedition 343, 343T and KR12-08 Scientists, Low coseismic friction on the Tohoku-oki fault determined from temperature measurements. *Science* ***342***, 1214-1217 (2013).

This research used samples and data provided by the International Ocean Discovery Program (IODP) that are under moratorium until 6 October 2017. After the moratorium data are accessible online and samples on request (www.iodp.org/access-data-and-samples). Seismic data were acquired by the Federal Institute for Geosciences and Natural Resources (BGR; Germany), data are jointly owned by Germany and Indonesian institutions. We sincerely thank all R/V JOIDES Resolution and IODP staff. L. Brandt and A. Mechler provided shipboard technical support for geochemical analysis. G. Spinelli and M. Lyle provided guidance regarding Si extraction. A. Hüpers, M. Torres and S. Owari conducted geochemical analysis and modeling, prepared figures, and wrote the manuscript; K. Milliken provided lithologic descriptions; T. Henstock and L. McNeill provided interpretation of seismic images; L. McNeill, B. Dugan, and K. Petronotis organized and managed the expedition; all authors contributed to the paper by providing shipboard measurements and scientific discussions. A. Hüpers acknowledges support by the Deutsche Forschungsgemeinschaft (HU1789/3-1). Two anonymous reviewers and associate editor Brent Grocholski are thanked for constructive reviews which improved the paper.

Figure captions:

Figure 1. Overview of study area and sampling locations. (A) Map of IODP Expedition 362 sites (red dots) and 2004 and 2005 rupture zones (modified from *29*). Red arrows and numbers show convergence vectors (cm/yr). White arrows and numbers indicate subduction velocities accounting for forearc motion (*30*). Yellow lines mark seismic profiles (*13, 15, 31*) where a high amplitude negative polarity (HANP) reflector is imaged or reported (yellow area). Dashed yellow line shows estimated extent of the HANP

reflector. (B) Seismic profile of the North Sumatran subduction inputs in the area of the drill sites, location is orange line in (A).

Figure 2. Depth profiles of key results from cored Sites U1480 (in red) and U1481 (in blue) showing simplified lithostratigraphy with lithologic units, sediment age, solid-phase amorphous SiO_2 (wt-%) and dissolved Cl concentration. Within unit III Cl concentrations drop to ~520 mM corresponding to increased amorphous silica content. Smear slide observations (Fig. S2) show biosilica and a homogeneous red-colored microcrystalline material, interpreted as a palagonite alteration product from volcanic ash, at 1250-1327 m below seafloor.

Figure 3. Modeling results of time- and temperature-dependent reaction kinetics and compaction in unit III from deposition to arrival at the subduction deformation front. 0 Myr is present time. (A) Combined fluid production from opal-A to opal-CT to quartz transition reaches the highest values close to Site U1480 with a double peak due to the onset of trench wedge sedimentation. The blue area shows the opal dehydration based on the possible range of bound water (2.1 - 12.1 wt.-%) (*22*). A minimum of 18 wt.-% opal-A is required to explain the observed freshening at Site U1480 assuming a high water content (12.1 wt.-%). Simulated dehydration of palagonite uses smectite to illite reaction kinetics as a proxy and peaks approximately 131 to 76 km seaward of the trench. Dehydration has been modeled for a final burial depth of 4 to 5 km for the base of unit III in the trench (red dashed and solid line, respectively). Weight percentages of 50 wt.-% and 100 wt.-% are assumed to show the potential range on fluid production. (B) Relative composition showing that opal-A transforms to quartz seaward of the subduction front. The smectite to illite transition (as a proxy for palagonite dehydration) should also be largely completed before subduction due to simulated temperatures of ~120 to 150°C using both 4 and 5 km sediment thickness in the trench, respectively (red dashed and solid line, respectively, shaded orange between).

Supplementary Materials:

Materials and Methods

Figures S1 to S6

Table S1

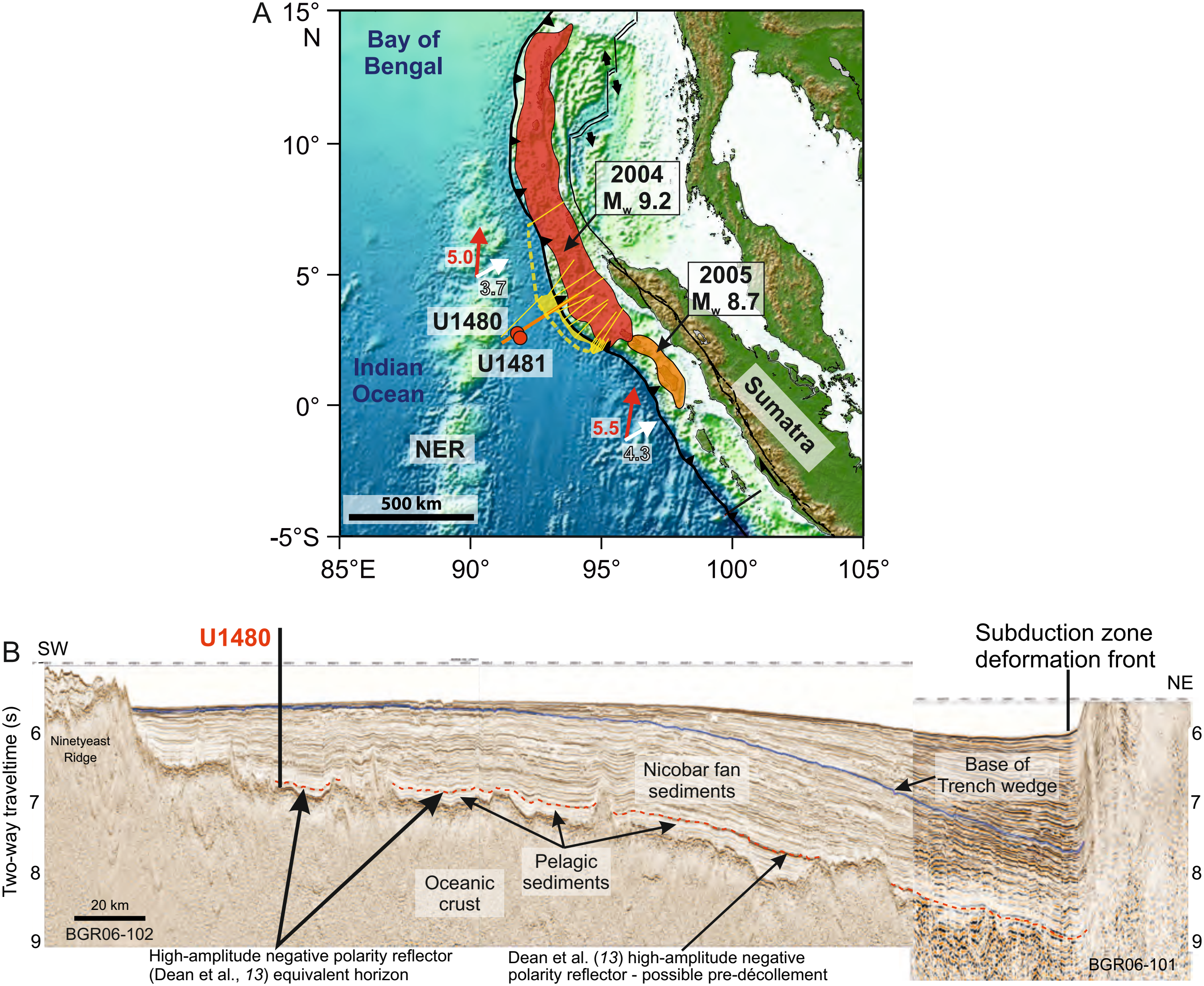
A
15° N
10°
5°
0°
-5°S
85°E
90°
95°
100°
105°
Bay of Bengal
2004 M$_w$ 9.2
2005 M$_w$ 8.7
5.0
3.7
U1480
U1481
Indian Ocean
Sumatra
5.5
4.3
NER
500 km
B
SW
U1480
Subduction zone deformation front
NE
Two-way traveltime (s)
6
7
8
9
Ninetyeast Ridge
Nicobar fan sediments
Base of Trench wedge
Pelagic sediments
Oceanic crust
20 km
BGR06-102
BGR06-101
High-amplitude negative polarity reflector (Dean et al., 13) equivalent horizon
Dean et al. (13) high-amplitude negative polarity reflector - possible pre-décollement

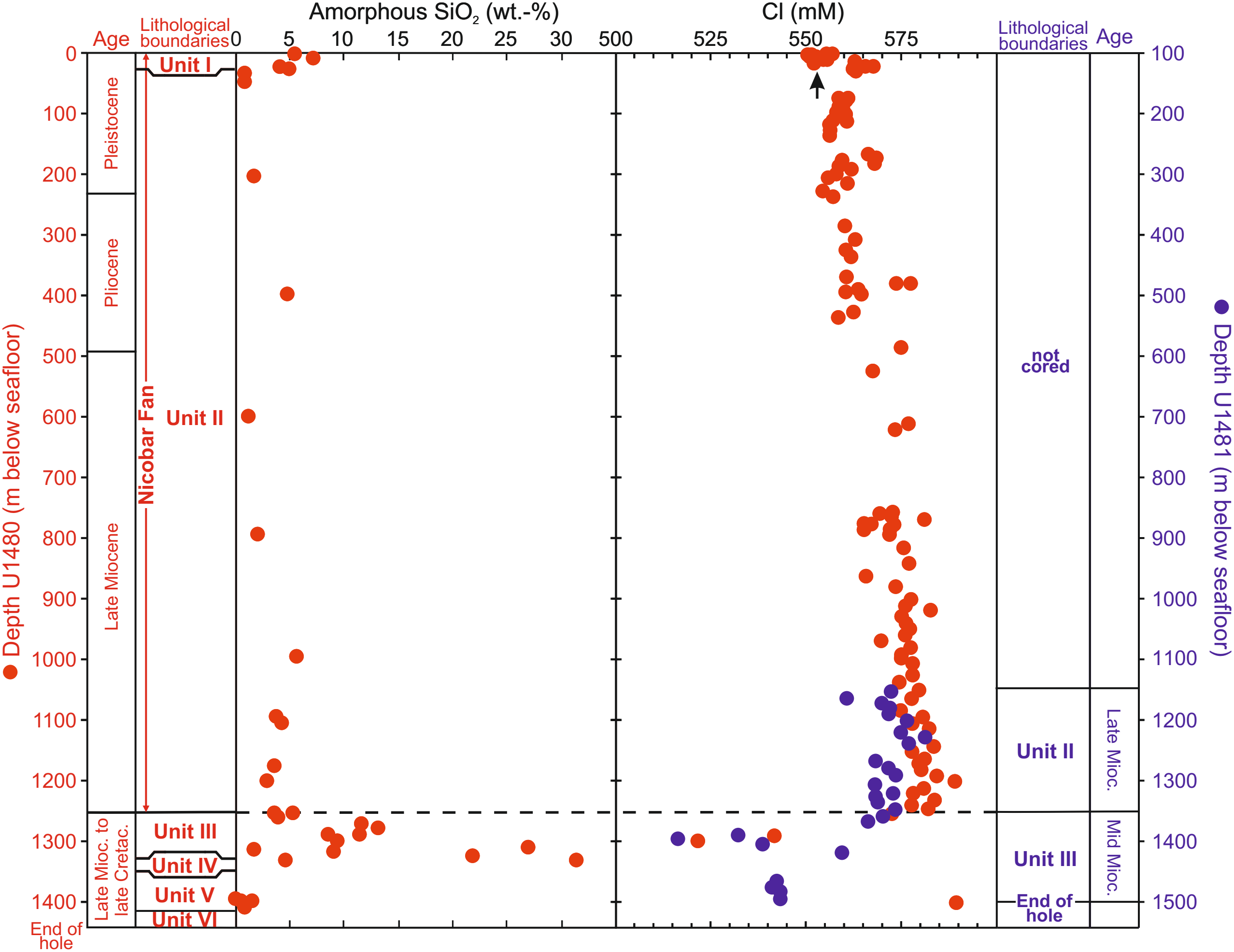
Amorphous SiO₂ (wt.-%)
0
5
10
15
20
25
30
Cl (mM)
500
525
550
575
Age
Lithological boundaries
Unit I
Pleistocene
Pliocene
Late Miocene
Nicobar Fan
Unit II
Late Mioc. to late Cretac.
Unit III
Unit IV
Unit V
Unit VI
End of hole
● Depth U1480 (m below seafloor)
0
100
200
300
400
500
600
700
800
900
1000
1100
1200
1300
1400
Lithological boundaries
Age
not cored
Unit II
Late Mioc.
Unit III
Mid Mioc.
End of hole
● Depth U1481 (m below seafloor)
100
200
300
400
500
600
700
800
900
1000
1100
1200
1300
1400
1500

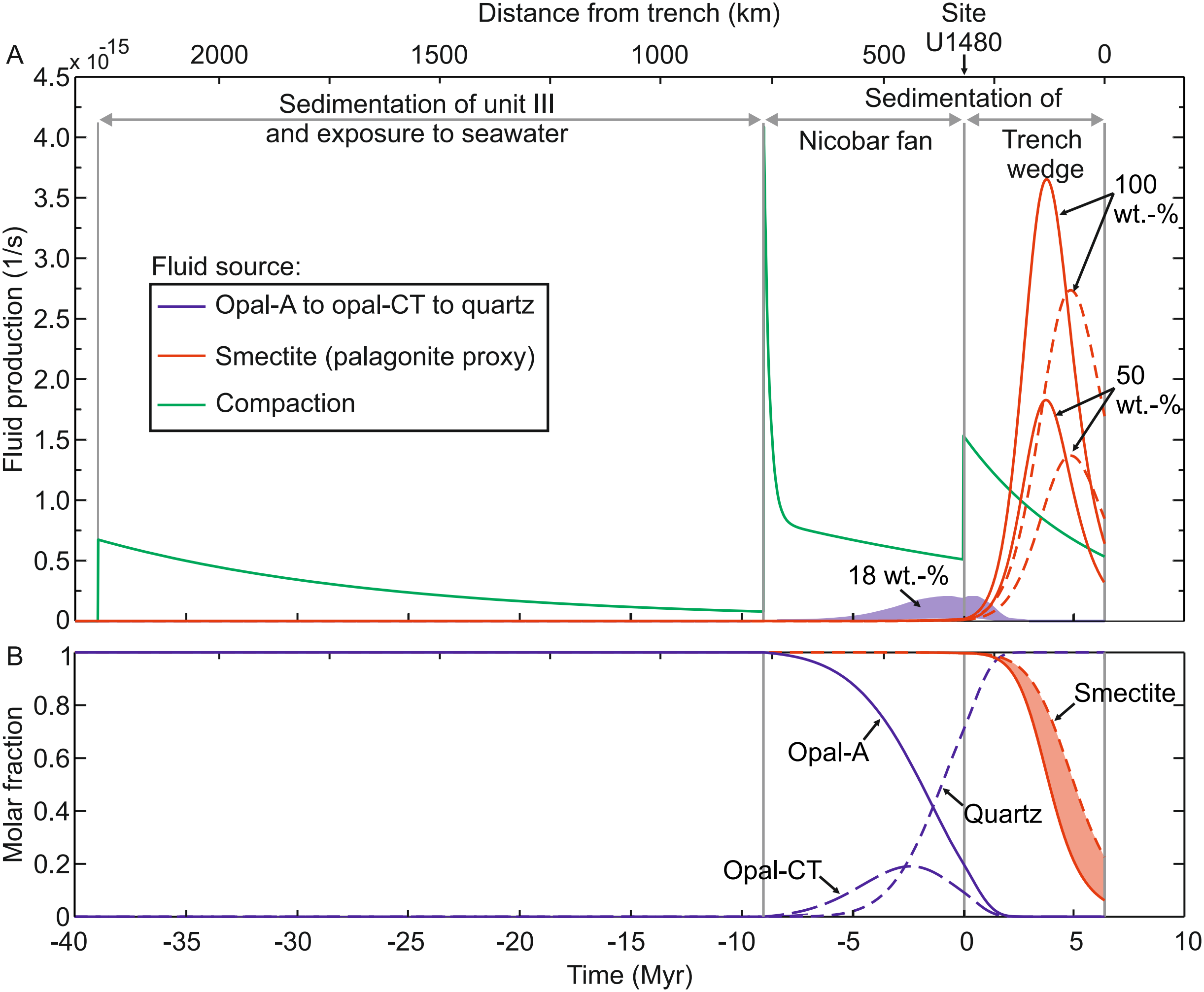
Distance from trench (km)
Site U1480
A
x 10^-15
2000
1500
1000
500
0
Sedimentation of unit III and exposure to seawater
Sedimentation of
Nicobar fan
Trench wedge
100 wt.-%
50 wt.-%
18 wt.-%
Fluid production (1/s)
4.5
4.0
3.5
3.0
2.5
2.0
1.5
1.0
0.5
0
Fluid source:
Opal-A to opal-CT to quartz
Smectite (palagonite proxy)
Compaction
B
Molar fraction
1
0.8
0.6
0.4
0.2
0
Smectite
Opal-A
Quartz
Opal-CT
-40
-35
-30
-25
-20
-15
-10
-5
0
5
10
Time (Myr)